JOC Article
pubs.acs.org/joc

Lower Rim 1,3-Diderivative of Calix[4]arene-Appended Salicylidene Imine (H_2L): Experimental and Computational Studies of the Selective Recognition of H_2L toward Zn^{2+} and Sensing Phosphate and Amino Acid by [ZnL]

Roymon Joseph, Jugun Prakash Chinta, and Chebrolu P. Rao*

Bioinorganic Laboratory, Department of Chemistry, Indian Institute of Technology Bombay, Mumbai 400 076, India

cprao@iitb.ac.in

Received March 10, 2010

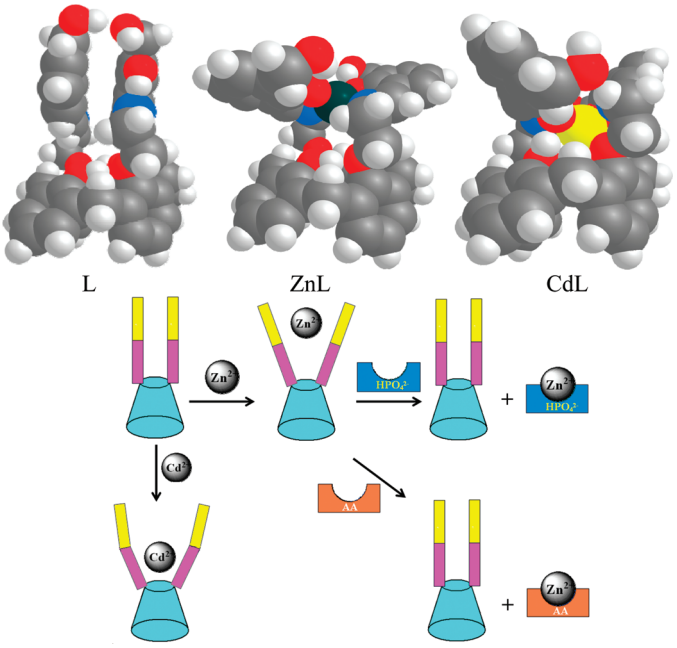

A new 1,3-diderivative of calix[4]arene appended with hydroxymethyl salicylyl imine has been synthesized and its ion recognition toward biologically relevant M^{n+} ions studied. The receptor H_2L showed selectivity toward Zn^{2+} by switch-on fluorescence among the 12 metal ions studied with a detection limit of 192 ppb. The interaction of Zn^{2+} with H_2L has been further supported by absorption studies, and the stoichiometry of the complex formed (1:1) has been established on the basis of absorption and ESI MS. Competitive ion titrations carried out reveal that the Zn^{2+} can be detected even in the presence of other metal ions of bioimportance. The mode of interaction of Zn^{2+} with conjugate has been established by a fleet of computational calculations carried out in a cascade manner, either on the ligand or on the complex, wherein the final optimizations were carried out by the density functional theory (DFT) and found that the Zn^{2+} and Cd^{2+} indeed bind differently. In situ prepared [ZnL] complex responds to both inorganic phosphate as well as AMP, ADP, and ATP with a minimum detection limit of 426 ppb wherein the Zn^{2+} from the complex is detached and recomplexed by the added phosphate moiety. It has been possible to build an INHIBIT logic gate for the conjugate using Zn^{2+} and HPO_4^{2-} as inputs by monitoring the fluorescence emission band at 444 nm as output. The amino acid sensing abilities of [ZnL] have been explored by fluorescence and absorbance spectroscopy where it showed selectivity toward Cys, Asp, and His through the formation of the Zn^{2+} complex of these amino acids by chelating through their side chain moieties. Thus, while H_2L is selective for Zn^{2+} among a number of cations, the [ZnL] is selective toward phosphate among a number of anions and also toward Asp, Cys, and His among the naturally occurring amino acids.

DOI: 10.1021/jo1004247 Published on Web 04/14/2010

Introduction

Zinc is one of the essential trace elements and second most abundant transition-metal ion present in human body. The zinc-containing proteins are abundant and act as both structural and functional proteins by exhibiting a wide range of biochemical activities.[1] The deficiency of Zn^{2+} ion in brain and pancreas may result in various disorders such as Parkinson's disease, epilepsy, and certain cancers.[2] In the proteins, Zn^{2+} is generally coordinated by selected amino acid side chains such as histidine, aspartic/glutamic acid, and cysteine while exhibiting high affinity toward phosphate.[1c,e] Thus, besides exhibiting a pivotal role in biology, the Zn^{2+} ions are associated with amino acids in their free or peptide form as well as anions including phosphate selectively. Both the amino acids and phosphates are indispensable in biology,[3] and the deficiency of these result in several side effects in humans.[4] Therefore, the selective recognition of the species such as Zn^{2+}, phosphate and amino acids are important in biology. It is always desirable to have one single molecular system that can provide features for recognition of all these kinds of species. Therefore, in the search for molecular systems which provide selectivity, conjugates of calixarenes are worthy of note, since these contain both a hydrophobic cavity and a hydrophilic rim and can also provide an ideal platform for the development of receptors toward ions or molecular species depending upon their functionalization.[5] Though some conjugates of calix[4]arene were demonstrated to have selectivity toward Zn^{2+} [6] or phosphate[7] or amino acids,[8] to our knowledge there has been no single calixarene-based receptor that recognizes all three of these components. Our research group has been involved in the synthesis of various calix[4]arene-appended amide- and imine-based conjugates for the selective sensing of ions and molecules.[6d,f,9] Recently, we have also explored the selective detection of amino acids using calix[4]arene derivatives bearing transition-metal ions.[8u,v] It is of interest to develop a calixarene-based molecular system that would recognize both the ions and molecules. Thus, in this paper, we discuss the synthesis and characterization of a calixarene conjugate (H_2L) that selectively recognizes Zn^{2+} and further involvement of the corresponding Zn^{2+} complex in the recognition of phosphate and amino acids. All the details of spectroscopy studies relevant to these aspects as well as the modeling the complexes of Zn^{2+} and Cd^{2+} are discussed in this paper.

Results and Discussion

The receptor molecule (H_2L) has been synthesized starting from *p-tert*-butylcalix[4]arene (4) followed by dinitrile (**5**) and then the diamine (**6**) derivative as shown in Scheme 1, as already reported by us as well by others in the literature.[6d,10] The receptor molecule has been synthesized by reacting the diamine derivative **6** with 5-*tert*-butyl-2-hydroxy-3-(hydroxymethyl)benzaldehyde (**3**) in methanol. In turn, **3** has been synthesized from *p-tert*-butylphenol (**1**) via 2,6-bis(hydroxymethyl)-4-*tert*-butylphenol (**2**).[11] The precursors and final products were characterized by analytical and spectral

(1) (a) Maret, W. *Biometals* **2001**, *14*, 187. (b) Blokesch, M.; Rohrmoser, M.; Rode, S.; Bock, A. *J. Bacteriol.* **2004**, *186*, 2603. (c) Karlin, S.; Zhu, Z. −Y. *Proc. Natl. Acad. Sci. U.S.A.* **1997**, *94*, 14231. (d) Baglivoa, I.; Russoa, L.; Esposito, S.; Malgieri, G.; Renda, M.; Salluzzo, A.; Blasio, B. D.; Isernia, C.; Fattorusso, R.; Pedone, P. V. *Proc. Natl. Acad. Sci. U.S.A.* **2009**, *106*, 6933. (e) McCall, K. A.; Huang, C.-C.; Fierke, C. A. *J. Nutr.* **2000**, *130*, 1437S. (f) Coleman, J. E. *Annu. Rev. Biochem.* **1992**, *61*, 897.

(2) (a) Ho, E. *J. Nutr. Biochem.* **2004**, *15*, 572. (b) Taylor, C. G. *Biometals* **2005**, *18*, 305.

(3) (a) Nelson, D.; Cox, M. M. *Principles of Biochemistry*, 4th ed.; W. H. Freeman: New York, 2004. (b) Voet, D., Voet, J. *Biochemistry*, 3rd ed.; John Wiley & Sons: New York, 2004. (c) Bodin, P.; Burnstock, G. *Neurochem. Res.* **2001**, *26*, 959. (d) Chakrabarti, P. *J. Mol. Biol.* **1993**, *234*, 463.

(4) (a) Puka-Sundvall, M.; Eriksson, P.; Nilsson, M.; Sandberg, M.; Lehmann, A. *Brain Res.* **1995**, *705*, 65. (b) Heafield, M. T.; Fearn, S.; Steventon, G. B.; Waring, R. H.; Williams, A. C.; Sturman, S. G. *Neurosci. Lett.* **1990**, *110*, 216. (c) Kelly, S. C.; O'Connell, P. J.; O'Sullivan, C. K.; Guilbault, G. G. *Anal. Chim. Acta* **2000**, *412*, 111. (d) Yefimenko, I.; Fresquet, V.; Marco-Marin, C.; Rubio, V.; Cervera, J. *J. Mol. Biol.* **2005**, *349*, 127. (e) Beutler, E. *Blood* **2008**, *111*, 16.

(5) (a) Kim, J. S.; Quang, D. T. *Chem. Rev.* **2007**, *107*, 3780. (b) Creaven, B. S.; Donlon, D. F.; McGinley, J. *Coord. Chem. Rev.* **2009**, *253*, 893. (c) Beer, P. D. *Acc. Chem. Res.* **1998**, *31*, 71. (d) Kim, H. J.; Kim, S. K.; Lee, J. Y.; Kim, J. S. *J. Org. Chem.* **2006**, *71*, 6611. (e) Gunnlaugsson, T.; Glynn, M.; Tocci, G. M.; Kruger, P. E.; Pfeffer, F. M. *Coord. Chem. Rev.* **2006**, *250*, 3094. (f) Lee, J. W.; Park, S. Y.; Cho, B.-K.; Kim, J. S *Tetrahedron Lett.* **2007**, *48*, 2541. (g) Breitkreuz, C. J.; Zadmard, R.; Schrader, T. *Supramol. Chem.* **2008**, *20*, 109. (h) Senthilvelan, A.; Ho, I.-T.; Chang, K.-C.; Lee, G.-H.; Liu, Y.-H.; Chung, W.-S. *Chem.—Eur. J.* **2009**, *15*, 6152.

(6) (a) Bagatin, I. A.; de Souza, E. S.; Ito, A. S.; Toma, H. E. *Inorg. Chem. Commun.* **2003**, *6*, 288. (b) Unob, F.; Asfari, Z.; Vicens, J. *Tetrahedron Lett.* **1998**, *39*, 2951. (c) Cao, Y.-D.; Zheng, Q.-Y.; Chen, C.-F.; Huang, Z.-T. *Tetrahedron Lett.* **2003**, *44*, 4751. (d) Dessingou, J.; Joseph, R.; Rao, C. P. *Tetrahedron Lett.* **2005**, *46*, 7967. (e) Joseph, R.; Ramanujam, B.; Pal, H.; Rao, C. P. *Tetrahedron Lett.* **2008**, *49*, 6257. (f) Pathak, R. K.; Ibrahim, S. M.; Rao, C. P. *Tetrahedron Lett.* **2009**, *50*, 2730. (g) Park, S. Y.; Yoon, J. H.; Hong, C. S.; Souane, R.; Kim, J. S.; Matthews, S. E.; Vicens, J. *J. Org. Chem.* **2008**, *73*, 8212.

(7) (a) Szemes, F.; Hesek, D.; Chen, Z.; Dent, S. W.; Drew, M. G. B.; Goulden, A. J.; Graydon, A. R.; Grieve, A.; Mortimer, R. J.; Wear, T.; Weightman, J. S.; Beer, P. D. *Inorg. Chem.* **1996**, *35*, 5868. (b) Kivlehan, F.; Macea, W. J.; Moynihan, H. A.; Arrigan, D. W. M. *Anal. Chim. Acta* **2007**, *585*, 154–160. (c) Evans, A. J.; Matthews, S. E.; Cowley, A. R.; Beer, P. D. *Dalton Trans.* **2003**, 4644. (d) Gale, P. A.; Chen, Z.; Drew, M. G. B.; Heath, J. A.; Beer, P. D. *Polyhedron* **1998**, *17*, 405. (e) Gupta, V. K.; Ludwig, R.; Agarwal, S. *Anal. Chim. Acta* **2005**, *538*, 213. (f) Quinlan, E.; Matthews, S. E.; Gunnlaugsson, T. *J. Org. Chem.* **2007**, *72*, 7497.

(8) (a) Zielenkiewicz, W.; Marcinowicz, A.; Cherenok, S.; Kalchenko, V. I.; Poznanski *J. Supramol. Chem.* **2006**, *18*, 167. (b) Arena, G.; Casnati, A.; Contino, A.; Magri, A.; Sansone, F.; Sciotto, D.; Ungaro, R. *Org. Biomol. Chem.* **2006**, *4*, 243. (c) Douteau-Guével, N.; Perret, F.; Coleman, A. W.; Morel, J. −P.; Morel-Desrosiers, N. *J. Chem. Soc., Perkin Trans. 2* **2002**, 524. (d) Douteau-Guével, N.; Coleman, A. W.; Morel, J. −P.; Morel-Desrosiers, N. *J. Chem. Soc., Perkin Trans. 2* **1999**, 629. (e) Perret, F.; Lazar, A. N.; Coleman, A. W. *Chem. Commun.* **2006**, 2425. (f) Selkti, M.; Coleman, A. W.; Nicolis, I.; Douteau-Guével, N.; Villain, F.; Tomas, A.; de Rango, C. *Chem. Commun.* **2000**, 161. (g) Lazar, A. N.; Danylyuk, O.; Suwinska, K.; Coleman, A. W. *J. Mol. Struct.* **2006**, *825*, 20. (h) Stone, M. M.; Franz, A. H.; Lebrilla, C. B. *J. Am. Soc. Mass Spectrum* **2002**, *13*, 964. (i) Perret, F.; Morel-Desrosiers, N.; Coleman, A. W. *J. Supramol. Chem.* **2002**, *2*, 533. (j) Douteau-Guevel, N.; Coleman, A. W.; Morel, J.-P.; Morel-Desrosiers, N. *J. Phys. Org. Chem.* **1998**, *11*, 693. (k) Da Silva, E.; Coleman, A. W. *Tetrahedron* **2003**, *59*, 7357. (l) Arena, G.; Contino, A.; Gulino, F. G.; Magri, A.; Sansone, F.; Sciotto, D.; Ungaro, R. *Tetrahedron Lett.* **1999**, *40*, 1597. (m) Frish, L.; Sansone, F.; Casnati, A.; Ungaro, R.; Cohen, Y. *J. Org. Chem.* **2000**, *65*, 5026. (n) Casnati, A.; Fabbi, M.; Pelizzi, N.; Pochini, A.; Sansone, F.; Ungaro, R. *Bioorg. Med. Chem. Lett.* **1996**, *6*, 2699. (o) Baldini, L.; Casnati, L.; Sansone, F.; Ungaro, R. *Chem. Soc. Rev.* **2007**, *36*, 254. (p) Ikeda, A.; Shinkai, S. *Chem. Rev.* **1997**, *97*, 1713. (q) Casnati, A.; Sansone, F.; Ungaro, R. *Acc. Chem. Res.* **2003**, *36*, 246. (r) Kalchenko, O. I.; Da Silva, E.; Coleman, A. W. *J. Inclusion Phenom. Macrocycl. Chem.* **2002**, *43*, 305. (s) Lu, J. Q.; Zhang, L.; Sun, T. Q.; Wang, G. X.; Wu, L. Y. *Chin. Chem. Lett.* **2006**, *17*, 575. (t) Li, H.; Wang, X. *Photochem. Photobiol. Sci.* **2008**, *7*, 694. (u) Chinta, J. P.; Acharya, A.; Kumar, A.; Rao, C. P. *J. Phys. Chem. B* **2009**, *113*, 125075. (v) Joseph, R.; Ramanujam, B.; Acharya, A.; Rao, C. P. *J. Org. Chem.* **2009**, *74*, 8181.

(9) (a) Joseph, R.; Ramanujam, B.; Acharya, A.; Rao, C. P. *Tetrahedron Lett.* **2009**, *50*, 2735. (b) Joseph, R.; Ramanujam, B.; Acharya, A.; Khutia, A.; Rao, C. P. *J. Org. Chem.* **2008**, *73*, 5745. (c) Joseph, R.; Ramanujam, B.; Pal, H.; Rao, C. P. *Tetrahedron Lett.* **2008**, *49*, 6257.

(10) (a) Collins, E. M.; McKervey, M. A.; Madigan, E.; Moran, M. B.; Owens, M.; Ferguson, G.; Harris, S. J. *J. Chem. Soc., Perkin Trans. 1* **1991**, 3137. (b) Joseph, R.; Gupta, A.; Rao, C. P. *Indian J. Chem., Sect A* **2007**, *46A*, 1095. (c) Zhang, W.-C.; Huang, Z.-T. *Synthesis* **1997**, 1073.

(11) (a) Amato, M. E.; Ballistreri, F. P.; Pappalardo, A.; Sciotto, D.; Tomaselli, G. A.; Toscano, R. M. *Tetrahedron* **2007**, *63*, 9751.

SCHEME 1. Synthesis of the Precursor Molecule 3 and Receptor Molecule H_2L[a]

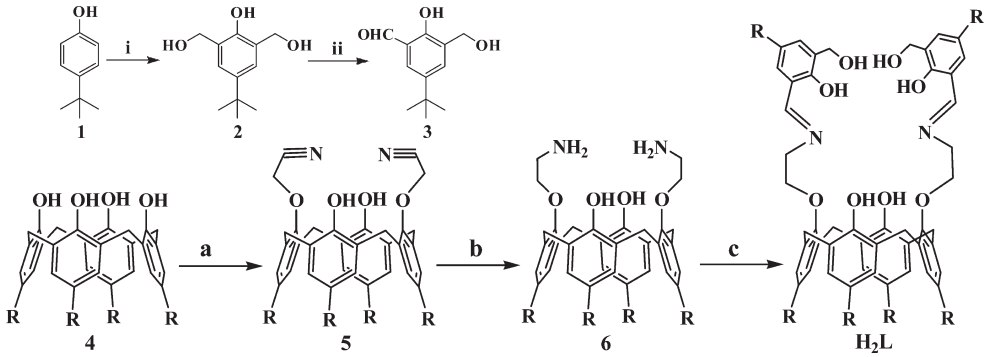

[a]Synthesis of the precursor molecule, **3** (top row): (i) NaOH, CH_2O, 7 d, rt, (ii) MnO_2, $CHCl_3$, 8 h, rt. Synthesis of the receptor molecule H_2L (bottom row): (a) K_2CO_3, $ClCH_2CN$, acetone, reflux for 7 h; (b) $LiAlH_4$, diethyl ether, reflux for 5 h; (c) **3**, CH_3OH, reflux. R = *tert*-butyl.

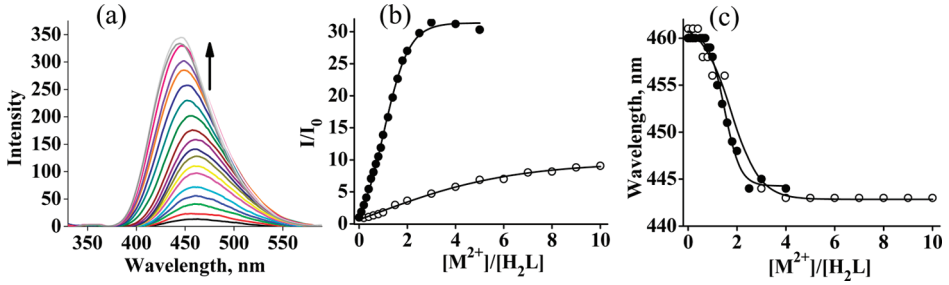

FIGURE 1. Fluorescence data for the titration of H_2L by Zn^{2+} and Cd^{2+} in methanol: (a) spectral traces obtained during the titration of H_2L with Zn^{2+}, (b) plot of relative fluorescence intensity (I/I_0) versus the mole ratio of $[M^{2+}]/[H_2L]$ added, and (c) plot of change in the wavelength versus the mole ratio of $[M^{2+}]/[H_2L]$ added. ● = Zn^{2+}; ○ = Cd^{2+}.

techniques (see the Experimental Section and Supporting Information).

The receptor molecule H_2L has been characterized satisfactorily by ^1H and ^{13}C NMR, IR, ESI MS, and elemental analysis. H_2L exhibits a ^1H NMR peak at 8.61 ppm characteristic of the CH=N proton. The protons of the bridged methylene were observed at 3.27 and 4.23 ppm owing to the diastereotopic coupling constant (J = 13.4 Hz) indicating the cone conformation.

A. Cation Recognition Studies. The binding, recognition, and selectivity of H_2L toward cations have been studied by absorption and fluorescence spectral titrations.

Fluorescence Titration. The receptor H_2L was excited at 320 nm, and its fluorescence emission was studied in the range 330−600 nm. All of the studies were carried out in methanol by maintaining the ligand concentration of 10 μM throughout the experiment and varying the mole ratio of the added metal ion. The metal ions subjected to the recognition studies were Mn^{2+}, Fe^{2+}, Co^{2+}, Ni^{2+}, Cu^{2+}, Zn^{2+}, Cd^{2+}, Hg^{2+}, Ca^{2+}, Mg^{2+}, Na^+, and K^+ as their perchlorate salts. H_2L is a weak emitter as its fluorescence is quenched due to the photoelectron transfer (PET) process from the lone pair of nitrogen to the salicylidene moiety. During the titration with Zn^{2+}, the fluorescence intensity of H_2L increases as a function of increase in the mole ratio of $[Zn^{2+}]/[H_2L]$ (Figure 1a) and exhibits a sigmoidal behavior, wherein the intensity is saturated at >3 equiv (Figure 1b). During the titration, the emission band maximum shifts progressively to exhibit a blue shift of ∼15 nm at saturation (Figure 1c), and the titration exhibits a stoichiometric behavior. While the midpoint of this sigmoidal plot corresponds to a 1:1 complex, at saturation the fluorescence enhancement is ∼30 fold. During the titration with Zn^{2+}, the metal ion is chelated through phenolic oxygen and the imine nitrogen, resulting in the utilization of lone pair of the nitrogen to block the PET and thereby the fluorescence enhancement. However, a similar titration carried out between H_2L and Cd^{2+} resulted in the fluorescence enhancement of only 10-fold even after addition of 10 equiv of this ion, and hence, Cd^{2+} is at least 3-fold less effective as compared to that of Zn^{2+}. There is about 12−15 nm shift toward blue as a function of addition of Zn^{2+} or Cd^{2+}, suggesting the complex formation between the conjugate and these ions. The sigmoidal plots obtained in these cases exhibit a midpoint ratio of 1:1 for L^{2-} to Zn^{2+} and 4:1 for L^{2-} to Cd^{2+}, in addition to a three-times higher enhancement observed with Zn^{2+} (Figure 1b). Thus, the selectivity difference observed between Zn^{2+} and Cd^{2+} is ∼9−10 fold. The binding affinities of Zn^{2+} and Cd^{2+} toward L^{2-} have been calculated from the Benesi−Hildebrand equation and found to have association constants of $2.7 \pm 0.1 \times 10^4$ and $3.6 \pm 0.6 \times 10^3$ M^{-1}, respectively, suggesting an ∼8 times higher magnitude of association of Zn^{2+} with L^{2-} as compared to the Cd^{2+}. All this seems to suggest that the selectivity is proportional to the binding strength. A minimum concentration of ∼192 ppb of Zn^{2+} has been detected by fluorescence studies carried out by keeping H_2L and Zn^{2+} at 1:1 and bringing appropriate dilutions (Supporting Information).

Titration by various M^{n+} ions, viz., Mn^{2+}, Fe^{2+}, Co^{2+}, Ni^{2+}, Cu^{2+}, Hg^{2+}, Na^+, K^+, Ca^{2+}, and Mg^{2+}, resulted in no or minimal change in the fluorescence intensity (Figure 2), suggesting that these ions are not recognized by H_2L.

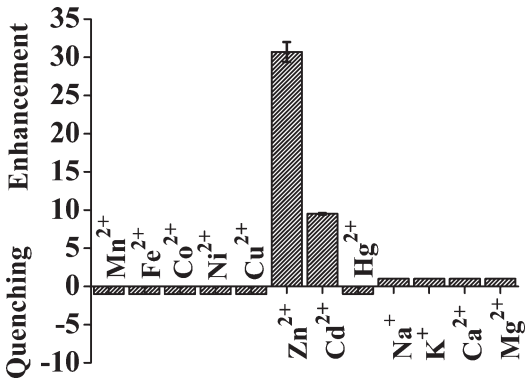

FIGURE 2. Histogram representing the fluorescence response of H_2L with different M^{n+} ions in methanol.

Therefore, both the shift observed in the emission maximum as well as the enhancement observed in the fluorescence intensity during the titration will allow one to use H_2L in the selective recognition of Zn^{2+}.

Competitive Ion Titration. In order to understand the practical applicability of H_2L in recognizing Zn^{2+} ions, competitive metal ion titrations were carried out in the presence of other M^{n+} ions. During the titration, the mole ratios of metal ions, viz., Na^+, K^+, Ca^{2+}, and Mg^{2+}, were kept constant at a 1:30 ratio with respect to H_2L, and the mole ratios of the added Zn^{2+} were varied. In case of other metal ions, *viz*., Mn^{2+}, Fe^{2+}, Co^{2+}, Ni^{2+}, Cu^{2+}, Cd^{2+} and Hg^{2+}, the ligand to metal ion ratio was kept at 1:5 and titrated against different equivalents of Zn^{2+}. It has been found that the added Zn^{2+} is able to replace all the other ions except Fe^{2+}, Cu^{2+}, and Hg^{2+} during the titration (Figure 3) and hence its use in the presence of other ions.

Computational Modeling of the Complexes of Zn^{2+} and Cd^{2+} by L^{2-}. Having observed from the fluorescence studies that the Zn^{2+} is about an order of magnitude more selective toward H_2L as compared to Cd^{2+}, computational calculations[12] were carried out as discussed in this paper. The initial model for the receptor molecule, H_2L was prepared from the published data of copper complex[13] by bringing the following modifications: (a) removing the copper center, (b) replacing *tert*-butyl moiety by hydrogen, (c) protonating the phenolate moieties, and (d) introducing a $-CH_2OH$ moiety ortho to the phenolic OH of the Schiff's base part of each of the arm. This has been optimized by going through a cascade process starting from PM3 → HF/STO-3G → HF/3-21G → HF/6-31G → B3LYP/3-21G → B3LYP/6-31G. The output

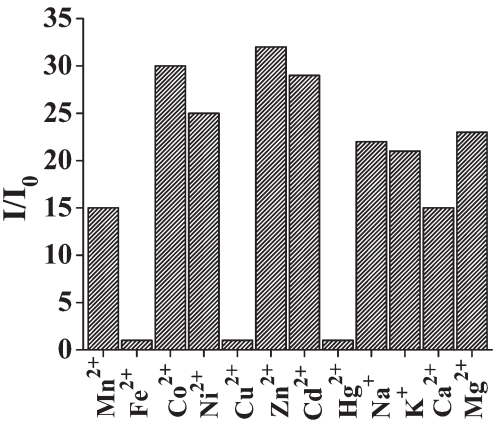

FIGURE 3. Plot of relative fluorescence intensity of H_2L with Zn^{2+} in the presence of 5 equiv of Mn^{2+}, Fe^{2+}, Co^{2+}, Ni^{2+}, Cu^{2+}, Cd^{2+}, and Hg^{2+} and 30 equiv of Na^+, K^+, Ca^{2+}, and Mg^{2+} in methanol.

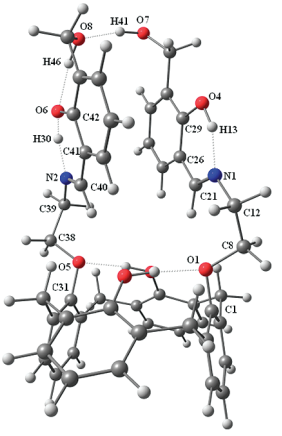

FIGURE 4. B3LYP/6-31G-optimized structure of H_2L stabilized through both the intra- and inter-arm hydrogen bonds. Data for these hydrogen bonds: (i) O6−H30···N2 hydrogen bond: N2···H30 = 1.479 Å, O6···N2 = 2.467 Å, O6−H30−N2 = 150.0°; (ii) O8−H46···O6 hydrogen bond: O6···H46 = 1.828 Å, O8···O6 = 2.641 Å, O8−H46−O6 = 137.3°; (iii) O7−H41···O8 hydrogen bond: O8···H41 = 1.759 Å, O7···O8 = 2.738 Å, O7−H41−O8 = 167.5°; (iv) O4−H13···N1 hydrogen bond: N1···H13 = 1.618 Å, O4···N1 = 2.545 Å, O4−H13−N1 = 147.7°.

obtained at every stage has been given as input for the next higher level of calculations. The optimized structure observed at B3LYP/6-31G level of calculation shows well ordered arms in an extended fashion wherein each arm is stabilized through phenolic O−H···N hydrogen bond interaction (intra-arm). In addition, one of the arms extend a weak hydrogen bond, viz., alcoholic O−H···O(phenolic). Further, the two arms are connected through a hydrogen bond formed between their alocoholic−OH groups (inter-arm), as can be seen from Figure 4. The hydrogen-bond interactions observed at the phenolic lower rim indicate the cone conformation; the inter-arm interactions also support that conformation.

In order to make the Zn^{2+} or Cd^{2+} complex, the structure of H_2L obtained at B3LYP/6-31G level has been taken and was deprotonated at its both the phenolic centers of the Schiff's base of the arms to form L^{2-}. The metal ion has been placed well above the arms of L^{2-} and was allowed to

(12) Frisch, M. J.; Trucks, G. W.; Schlegel, H. B.; Scuseria, G. E.; Robb, M. A.; Cheeseman, J. R.; Montgomery, J. A., Jr.; Vreven, T.; Kudin, K. N.; Burant, J. C.; Millam, J. M.; Iyengar, S. S.; Tomasi, J.; Barone, V.; Mennucci, B.; Cossi, M.; Scalmani, G.; Rega, N.; Petersson, G. A.; Nakatsuji, H.; Hada, M.; Ehara, M.; Toyota, K.; Fukuda, R.; Hasegawa, J.; Ishida, M.; Nakajima, T.; Honda, Y.; Kitao, O.; Nakai, H.; Klene, M.; Li, X.; Knox, J. E.; Hratchian, H. P.; Cross, J. B.; Bakken, V.; Adamo, C.; Jaramillo, J.; Gomperts, R.; Stratmann, R. E.; Yazyev, O.; Austin, A. J.; Cammi, R.; Pomelli, C.; Ochterski, J. W.; Ayala, P. Y.; Morokuma, K.; Voth, G. A.; Salvador, P.; Dannenberg, J. J.; Zakrzewski, V. G.; Dapprich, S.; Daniels, A. D.; Strain, M. C.; Farkas, O.; Malick, D. K.; Rabuck, A. D.; Raghavachari, K.; Foresman, J. B.; Ortiz, J. V.; Cui, Q.; Baboul, A. G.; Clifford, S.; Cioslowski, J.; Stefanov, B. B.; Liu, G.; Liashenko, A.; Piskorz, P.; Komaromi, I.; Martin, R. L.; Fox, D. J.; Keith, T.; Al-Laham, M. A.; Peng, C. Y.; Nanayakkara, A.; Challacombe, M.; Gill, P. M. W.; Johnson, B.; Chen, W.; Wong, M. W.; Gonzalez, C.; Pople, J. A. *Gaussian 03, Revision C.02*; Gaussian, Inc., Wallingford CT, **2004**.

(13) Dey, M.; Rao, C. P.; Guionneau, P. *Inorg. Chem. Commun.* **2005**, *8*, 998.

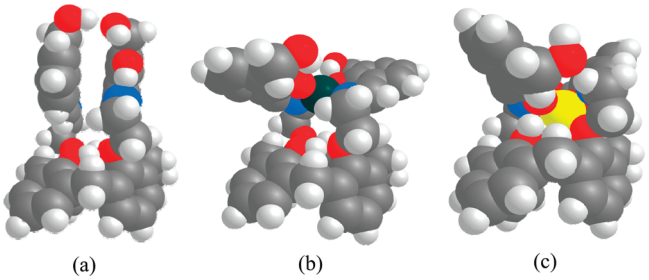

FIGURE 5. Space-filling models: (a) B3LYP/6-31G-optimized structure of H_2L, (b) B3LYP/LanL2DZ-optimized structure of [ZnL], and (c) B3LYP/LanL2DZ-optimized structure of [CdL].

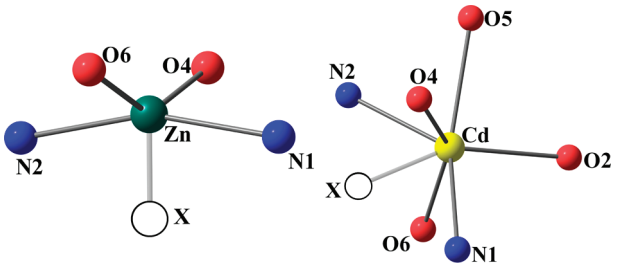

FIGURE 6. Coordination cores of [ZnL] and [CdL]. The unfilled circle "X" represents the vacant site. Metric data for [ZnL]: N1−Zn = 2.071, N2−Zn = 2.072, O6−Zn = 1.979, O4−Zn = 1.979 Å; N2−Zn−N1 = 161.7, N2−Zn−O6 = 91.3, N2−Zn−O4 = 94.8, N1−Zn−O6 = 94.8, N1−Zn−O4 = 91.3, O6−Zn−O4 = 141.5°. The metric data for [CdL]: N1−Cd = 2.377, N2−Cd=2.323, O2−Cd = 2.445, O4−Cd = 2.325, O5−Cd=2.441 and O6−Cd = 2.229 Å; N1−Cd−O5 = 147.4, N1−Cd−O2 = 98.5, N1−Cd−O4 = 76.8, N1−Cd−N2 = 129.2, N1−Cd−O6 = 84.6, O2−Cd−O5 = 82.7, N2−Cd−O2 = 125.5, N2−Cd−O4 = 91.0, N2−Cd−O5 = 70.6, N2−Cd−O6 = 79.1, O2−Cd−O6 = 81.2, O2−Cd−O4 = 128.9, O4−Cd−O5 = 77.3, O4−Cd−O6 = 146.2, O5−Cd−O6 = 127.4°.

minimize. The minimization in the presence of metal ion was carried out in a cascade fashion starting from PM3 → HF/STO-3G → HF/3-21G → HF/6-31G → B3LYP/3-21G → B3LYP/6-31G → B3LYP/LanL2DZ in the case of zinc and HF/STO-3G → HF/3-21G → B3LYP/3-21G → B3LYP/LanL2DZ in the case of cadmium. Such minimizations resulted in the formation of Zn^{2+} or Cd^{2+} complex by breaking the hydrogen-bonding interactions present between the two arms. The Zn^{2+} interacts primarily at the Schiff's base core, and the Cd^{2+} primarily interacts at the lower rim phenolic core (Figure 5).

The Zn^{2+} showed a distorted four-coordination geometry bonded through two imine nitrogens and two Schiff's base phenolic oxygens. The Cd^{2+} showed a distorted six coordination geometry bonded through two imine nitrogens, two Schiff's base phenolic oxygens, and two lower rim phenolic groups (Figure 6). The Zn−O and Zn−N were found to have distances of 1.979 and 2.072 Å, respectively, distance which were commonly found in the literature. The coordination angles observed with the Zn^{2+} core provides a better fit if it were to be considered as a trigonal bipyramidal with one trigonal center being vacant, where the trans-angle, viz., N1−Zn−N2, is found to be 162°. The Cd−O and Cd−N distances were found to be in the range 2.229−2.445 and 2.323−2.377 Å, respectively, the distances which were commonly found in the literature.[14] The coordination angles observed with the Cd^{2+} core provide a better fit if it were to be considered as a seven-coordinated capped octahedral structure with one vacant site. The [ZnL] exhibits at least 40 kcal/mol higher stabilization energy as compared to that of the [CdL] complex at the same level of DFT calculations. On going from H_2L → [ZnL] → [CdL], the conformations of the arms vary progressively to accommodate the corresponding metal ion by providing appropriate coordination. The list of conformational angles given in Table 1 clearly indicate that a major conformational change was observed with the C−N bond (Supporting Information).

(14) Xu, X.-Y.; Chen, J.-L.; Luo, Q.-H.; Shen, M.-C.; Haung, X.-Y.; Wu, Q.-J. *Polyhedron* **1997**, *16*, 223.

TABLE 1. Conformational Angles (deg) of the Arms Obtained upon Optimization for H_2L and Its Zn^{2+} and Cd^{2+} Complexes

	H_2L		[ZnL]		[CdL]	
	arm-1	arm-2	arm-1	arm-2	arm-1	arm-2
C1−O1−C8−C12	−156	−169	−178	−178	−170	177
O1−C8−C12−N1	−74	−77	−64	−64	−57	−49
C8−C12−N1−C21	23	47	−73	−73	−101	−125
C12−N1−C21−C26	179	176	−179	−179	177	177
N1−C21−C26−C29	−0.8	−3	3	3	−7	−5
C21−C26−C29−O4	2	4	1	1	1	1

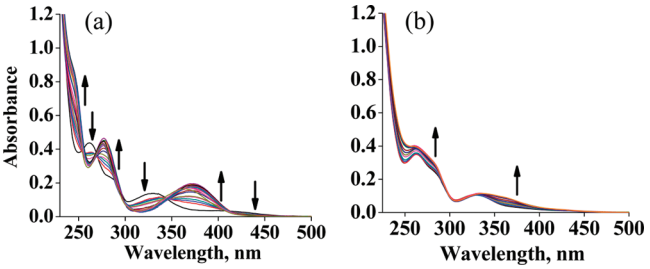

FIGURE 7. Absorption spectra obtained during the titration of H_2L with (a) Zn^{2+} and (b) Cd^{2+} in methanol.

Absorption Titration. Absorption titrations were also carried out to support the binding of Zn^{2+} with H_2L. During the titration, the concentration of H_2L was kept constant at 20 μM and the mole ratio of Zn^{2+} was varied. Addition of Zn^{2+} to a solution of H_2L in methanol brought changes in its absorption spectra with six absorption bands observed at 375, 320, 277, 262, 247, and 435 nm (Figure 7a). When H_2L was titrated against Zn^{2+}, a marginal increase was observed in the absorbance of the bands at 375, 277, and 247 nm and a significant decrease in the bands at 320, 262, and 435 nm. Five isosbestic points were observed at 412, 345, 295, 269, and 255 nm, and all these clearly indicate the complex formation of H_2L with Zn^{2+}. Absorption bands of the conjugate obtained at 261 and 330 nm have been shifted to 277 and 370 nm, respectively, in the presence of Zn^{2+}. A plot of absorbance versus mole ratio, $[Zn^{2+}]/[H_2L]$, has been given in Figure 8a,b.

When similar titrations were carried out with Cd^{2+}, no isosbestic point was observed, except for a slight increase in the absorbance at 250 and 365 nm; however, this increase is much less than that observed in the case of Zn^{2+} (Figures 7b and 8c). In the case of the 263 nm band, the two ions exhibit opposite trends in their absorbance. Such absorption spectral changes observed with Cd^{2+} seem to indicate a different

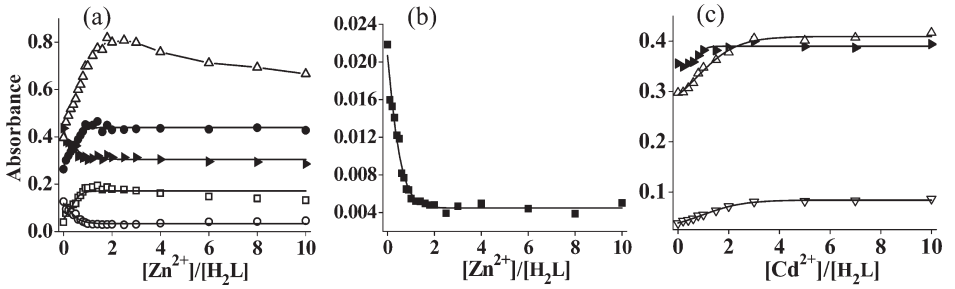

FIGURE 8. Absorption spectral data for the titration of H_2L with Zn^{2+} and Cd^{2+} in methanol: (a) and (b) are the plots of absorbance vs. mole ratio of ($[Zn^{2+}]/[H_2L]$) and (c) similar plots in case of Cd^{2+}. Symbols in figure (a) and (b) corresponds to □ = 375, ○ = 320, ● = 277, right-tilted solid triangle = 262, △ = 247, ■ = 435 nm and the symbols in figure (c) corresponds to ▽ = 365, right-tilted solid triangle = 263, △ = 250 nm.

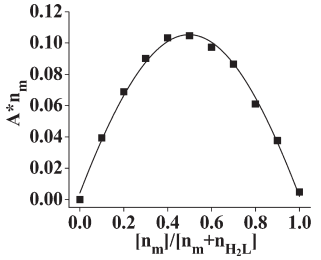

FIGURE 9. Job's plot obtained from the absorption titration of H_2L with Zn^{2+} in methanol, where A is the absorbance and n_m and n_{H2L} are the mole fractions of Zn^{2+} and H_2L, respectively.

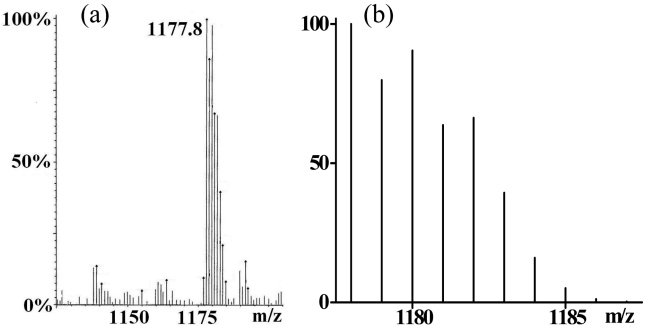

FIGURE 10. Mass spectral peak observed for the 1:1 complex of H_2L and Zn^{2+}: (a) experimental; (b) calculated.

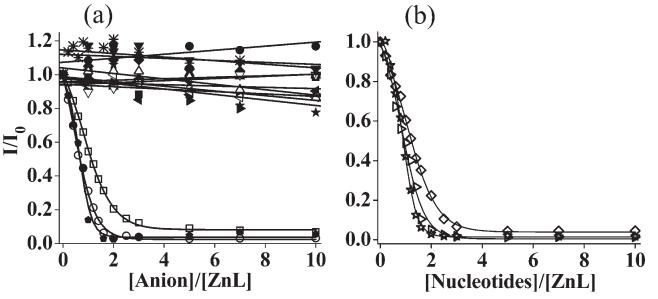

FIGURE 11. (a) Plot of relative fluorescence intensity (I/I_0) of [ZnL] with added anions and (b) similar plots with nucleotides, viz., AMP, ADP, and ATP in methanol. ■ = F^-, ● = Cl^-, ▲ = Br^-, ▼ = I^-, left-tilted solid triangle = ClO_4^-, right-tilted solid triangle = BF_4^-, ♦ = AcO^-, ▽ = SCN^-, left-tilted open triange = CO_3^{2-}, ★ = HCO_3^-, △ = NO_3^-, ∗ = SO_4^{2-}, ○ = $H_2PO_4^-$, □ = HPO_4^{2-}, solid pentagon = PO_4^{3-}, ◊ = AMP, right-tilted open triangle = ADP, and ☆ = ATP.

mode of binding of L^{2-} with Cd^{2+} as compared to that observed for Zn^{2+}. Even the absorption spectral studies resulted in association constants of $3.3 \pm 0.1 \times 10^4$ and $4.4 \pm 0.4 \times 10^3\ M^{-1}$, respectively, for Zn^{2+} and Cd^{2+} and are in agreement with those derived from the fluorescence data. Even the DFT studies showed higher stabilization energy of the formation of the complex in the case Zn^{2+} as compared to that with Cd^{2+}. Thus, both the absorption and fluorescence studies clearly supported strong affinity of Zn^{2+} toward H_2L as compared to that of Cd^{2+}. The stoichiometry of the complex formed was found to be 1:1 as derived from the Job's plot given in Figure 9. This has been further supported by ESI MS as reported in this paper.

Formation of [ZnL] by ESI MS. Mass spectral peak corresponding to the 1:1 complex of the conjugate and Zn^{2+} has been observed as isotopic multiplet centered about m/z = 1178.9 and is spread in the m/z values of 1177.8−1184.8. The presence of zinc ion in the complex is evident from the observed isotopic peak pattern (Figure 10).

B. Anion Recognition Studies. Since the receptor molecule detects Zn^{2+} selectively, the in situ prepared [ZnL] complex has been used for its anion recognition studies.

Fluorescence Titration. The anion recognition studies have been carried out by titrating an in situ generated complex, [ZnL], by different anions, viz., F^-, Cl^-, Br^-, I^-, ClO_4^-, BF_4^-, AcO^-, SCN^-, CO_3^{2-}, HCO_3^-, NO_3^-, SO_4^{2-}, $H_2PO_4^-$, HPO_4^{2-}, and PO_4^{3-}. All the anion titrations exhibited no significant change in the fluorescence intensity except those based on phosphate. During the titration with phosphate, the initially observed fluorescence intensity of [ZnL] has been found to be quenched gradually to reach an intensity that is similar to that of H_2L. The corresponding fluorescence behavior can very well be fitted to a sigmoidal type, and the inflection point corresponds to 1:1 (Figure 11a). Thus, out of the 15 anions studied, only $H_2PO_4^-$, HPO_4^{2-}, and PO_4^{3-} exhibited changes in the fluorescence intensity and all other ions exhibited no significant change. Since the Zn^{2+} complex of H_2L was found to be sensitive toward phosphate ions, fluorescence titrations were extended to biorelevant molecules possessing phosphate moiety, viz., adenosine monophosphate (AMP), adenosine diphosphate (ADP), and adenosine triphosphate (ATP). The titrations carried out with these nucleotides exhibited changes in the fluorescence intensity similar to that shown by simple inorganic phosphates (Figure 11b). The fluorescence quenching observed in the titration of the complex with phosphate is attributable to the removal of Zn^{2+} ions from the complex by the phosphate ions. The minimum concentration of HPO_4^{2-} that can be detected by [ZnL] has been found to be 426 ppb.

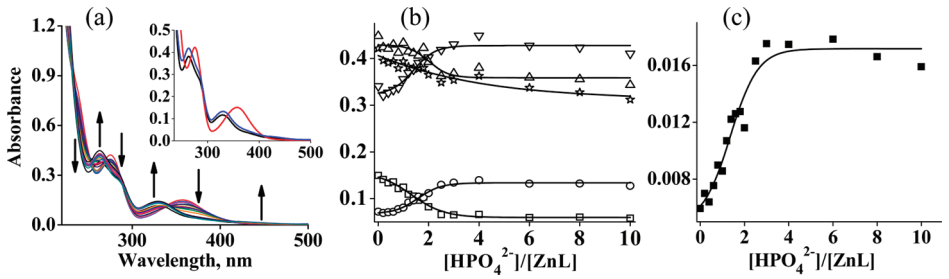

FIGURE 12. Absorption spectral data for the titration of [ZnL] with HPO_4^{2-} in methanol. (a) Spectra obtained during the titration; inset shows the absorption spectral traces corresponds to H_2L (black), [ZnL] (red) and [ZnL] with HPO_4^{2-} (blue); (b, c) Plots of absorbance vs mole ratio of HPO_4^{2-} added. △ = 250, ▽ = 263, ☆ = 276, ○ = 325, □ = 360, ■ = 435 nm.

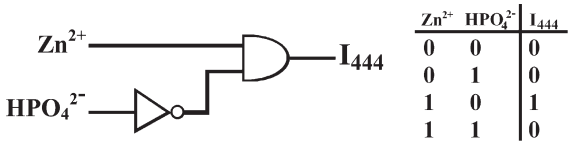

Zn^{2+}	HPO_4^{2-}	I_{444}
0	0	0
0	1	0
1	0	1
1	1	0

FIGURE 13. (a) INH logic gate represented using a conventional gate notation; an active output signal is obtained when Zn^{2+} = 1 and HPO_4^{2-} = 0. (b) Truth table for the INH logic gate; Zn^{2+} and HPO_4^{2-} are inputs to the system; I_{444} is the output signal of H_2L at 444 nm.

Absorption Titration. In order to understand the removal of Zn^{2+} by phosphate ions, absorption titrations were carried out. During the titration of the [ZnL] by HPO_4^{2-} (Figure 12), the absorption bands observed at 358 and 275 nm arising from the precursor complex have been progressively shifted to 330 and 264 nm, respectively, and the shifted bands correspond to that of free L. All this suggests the disruption of the [ZnL] complex followed by the removal of Zn^{2+} by the HPO_4^{2-} ions to result in free conjugate. It has been noted from the mole ratio versus absorbance plot (Figure 12b,c) that the changes observed for different bands during the titration between the [ZnL] and HPO_4^{2-} is exactly reverse to that observed during the titration of H_2L with Zn^{2+} (Figure 8a,b). This suggests a displacement mechanism during the titration of HPO_4^{2-}. Similar observations were noticed even with $H_2PO_4^-$, PO_4^{3-}, AMP, ADP, and ATP (Supporting Information).

INHIBIT Logic Gate. Logic gate properties of receptor molecule have also been explored by using Zn^{2+} and HPO_4^{2-} as input signals and the fluorescence emission response of H_2L at 444 nm monitored as output. In the absence of two inputs, the output signal showed a fluorescence quench for the emission band at 444 nm. H_2L did not exhibit any response in the presence of simple HPO_4^{2-} without addition of Zn^{2+}. The fluorescence intensity of H_2L has been increased upon the addition of 2 equiv of Zn^{2+} and resulted in an output signal at 444 nm. There was no output signal observed in the presence of equimolar solutions of both Zn^{2+} and HPO_4^{2-} in methanol. Hence, these studies suggests that H_2L can be used as an INHIBIT logic gate toward Zn^{2+} in the absence of HPO_4^{2-} by monitoring the fluorescence enhancement at 444 nm (Figure 13).

C. Amino Acid Recognition Studies. Since Zn^{2+} has the ability to form complexes with amino acids, in situ prepared [ZnL] has been used for the recognition of amino acids by fluorescence and absorption titrations.

Fluorescence Titration. The complex [ZnL] was titrated with the 20 naturally occurring amino acids which resulted in

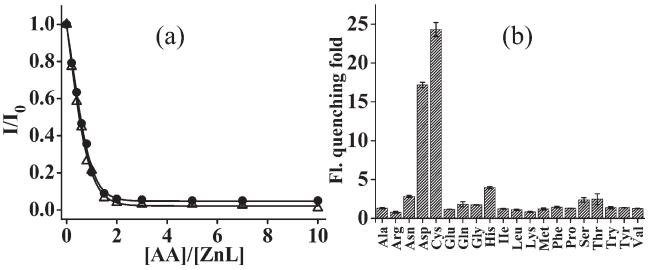

FIGURE 14. (a) Plot of relative fluorescence intensity (I/I_0) of [ZnL] versus the mole ratio of added Cys and Asp. (b) Histogram representing the fluorescence quenching fold caused by the titration of amino acids with [ZnL] (2:1) in methanol. ● = Asp and △ = Cys.

fluorescence quenching to different extents depending upon the chelation ability of the added amino acid toward Zn^{2+} (Figure 14). [ZnL] showed a maximum fluorescence quenching with some amino acids, and this follows a trend, Cys > Asp ≫ His. In fact, these are the three amino acids present to the maximum extent in the coordination sphere by binding through their side chains, viz., thiolato, carboxylate, and imidazolate, in zinc enzymes. A quick search of the 94 catalytic centers present in different zinc enzymes suggests that 50% of the coordination sphere is occupied by His, 20% by the carboxylate of Asp and Glu, and ~13−15% by Cys. Fluorescence quenching observed in the presence of these amino acids can be attributed mainly to the protonation of the Zn^{2+} coordination sphere followed by the formation of a complex of Zn^{2+} with the amino acid. This suggests that both the pK_a as well as the ability to chelate Zn^{2+} using the side chain are the major factors responsible for the observations.[8u] The dechelation of Zn^{2+} from [ZnL] by amino acids has been further confirmed by the absorption titration.

Absorption Titration. Upon titration of [ZnL] with Cys, the initial absorption bands of [ZnL] exhibited a red shift in the absorption maximum, and the spectra obtained after 2 equiv addition of Cys are similar to that of the simple H_2L (Figure 15a). Therefore, the changes observed during the titration of phosphate and amino acids are similar to each other, and [ZnL] senses both these species through a displacement mechanism. Titrations carried out with Asp and His also resulted in the release of H_2L (Figure 15b).

Conclusions and Correlations

The salicylyl imine conjugate of calix[4]arene (H_2L) reported in this paper possesses an additional CH_2OH group

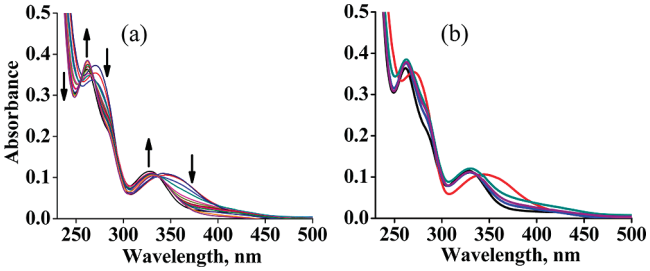

FIGURE 15. (a) Absorption spectra of L during the titration of [ZnL] with Cys. (b) Absorption spectra of H_2L (black), [ZnL] (red), {[ZnL] + Cys} (blue), {[ZnL] + Asp} (green), and {[ZnL] + His} (purple). The mole ratio of H_2L, Zn^{2+}, and amino acid was 1:2:2, and the solvent used was methanol.

when compared to a simple naphthyl derivative.[6d] This conjugate shows better selectivity toward Zn^{2+} among the 12 metal ions studied by fluorescence spectroscopy. Metal ion binding of the receptor molecule with Zn^{2+} has been further supported by absorption titration, and the new species of formation was demonstrated from the observed isosbestic points. There is a blue shift of ~15 nm observed in the emission band of the ligand when titrated with Zn^{2+}. Competitive titrations suggest the feasibility of sensing Zn^{2+} by H_2L even in the presence other biologically relevant metal ions, except Fe^{2+}, Cu^{2+}, and Hg^{2+}. ESI MS spectroscopy and the Job's plot suggest the formation of a 1:1 complex between L^{2-} and Zn^{2+}, and the fluorescence studies reveal a lowest detection limit of 192 ppb of Zn^{2+}. Thus, H_2L can act as fluorescence switch on sensor to Zn^{2+}.

The experimentally observed higher selectivity of H_2L toward Zn^{2+} over Cd^{2+} has been addressed by DFT calculations and found to have a different binding site in H_2L for each of these ions. While Zn^{2+} binds at the Schiff's base region by exhibiting a N_2O_2 core to result in trigonal bipyramidal geometry with one vacancy, the Cd^{2+} binds primarily at the lower rim by exhibiting a N_2O_4 core to result in capped octahedral geometry with one vacancy. In order to accommodate either Zn^{2+} or Cd^{2+}, the arms of H_2L needs to undergo appropriate conformational changes. In the case of H_2L, the two salicylyl moieties on the arms of calixarene are oriented parallel to each other and also parallel to the central axis of calix[4]arene scaffold. Upon complexation with Zn^{2+} or Cd^{2+}, the phenyl moieties orient themselves almost perpendicular to the central axis of the calixarene platform as a result of the major conformational change brought about the C−N of the arm. As the extent of conformational changes occurred differ between the Zn^{2+} and Cd^{2+} cases, their binding regions in H_2L also differ.

The in situ prepared [ZnL] complex can sense phosphate among the 15 anions studied by fluorescence and absorption spectroscopy. The response of nucleotides to the [ZnL] has also been established by spectroscopic studies resulting in the fluorescence quenching that is same as that of inorganic phosphates. During the anion titration, only phosphate could dechelate Zn^{2+} from [ZnL] and release the free H_2L, and the Zn^{2+} ion in turn is complexed by the phosphate. Hence, the present study unambiguously proves the use of H_2L as a sensor for Zn^{2+} and the corresponding [ZnL] as a selective phosphate sensor. The detection limit observed for HPO_4^{2-} with [ZnL] has been found to be 426 ppb. H_2L

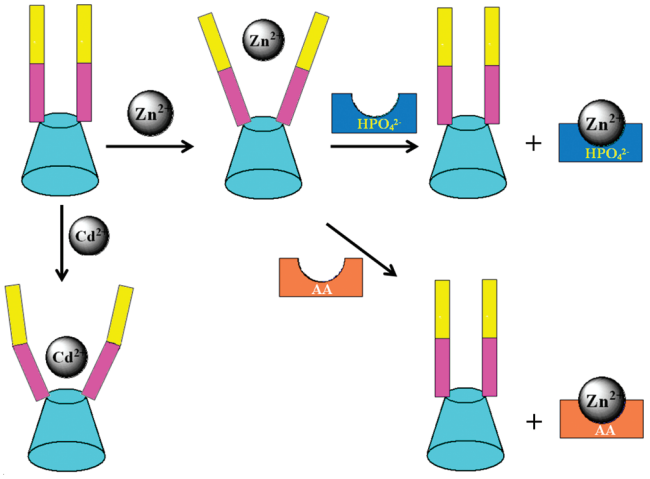

FIGURE 16. Cartoon representation of ion binding by H_2L and the reactivity of [ZnL] toward HPO_4^{2-} and amino acids.

exhibits INHIBIT logic gate properties when the inputs are Zn^{2+} and HPO_4^{2-} and the out put is the fluorescence emission intensity observed at 444 nm.

Interaction of [ZnL] with naturally occurring amino acids has been demonstrated by spectroscopic techniques that resulted in dechelation of Zn^{2+} from the complex of [ZnL] and the formation of the amino acid complex of zinc, as reflected from the emission and the absorption spectral studies. The fluorescence spectra obtained during the titration indicates that the rate of dechelation directly depends on the nature of the amino acid. Therefore, in this paper we demonstrate the ability of H_2L as a sensor for Zn^{2+} and further the use of [ZnL] as a sensor for phosphate. The [ZnL] also exhibits sensitivity primarily toward Cys and Asp which chelates Zn^{2+}. All these events have been pictorially depicted in Figure 16.

Experimental Section

Materials. All the perchlorate salts, viz., $Mn(ClO_4)_2 \cdot 6H_2O$, $Fe(ClO_4)_2 \cdot xH_2O$, $Co(ClO_4)_2 \cdot 6H_2O$, $Ni(ClO_4)_2 \cdot 6H_2O$, $Cu(ClO_4)_2 \cdot 6H_2O$, $Zn(ClO_4)_2 \cdot 6H_2O$, $Cd(ClO_4)_2 \cdot H_2O$, $Hg(ClO_4)_2 \cdot xH_2O$, $Na(ClO_4)_2 \cdot H_2O$, $K(ClO_4)_2$, $Ca(ClO_4)_2 \cdot 4H_2O$, and $Mg(ClO_4)_2 \cdot 6H_2O$, were procured from a US commercial supplier. Salts possessing different anions, viz., Bu_4NF, Me_4NCl, Bu_4NBr, Bu_4NI, Bu_4NClO_4, $Bu_4NH_2PO_4$, Na_2HPO_4, Na_3PO_4, NaSCN, NaOAc, Na_2SO_4, Na_2CO_3, $NaHCO_3$, $NaNO_3$, and $NaBF_4$ were procured from a commercial supplier in India. All the amino acids and nucleotides were purchased from the same source in India. Materials used for the synthesis of *p-tert*-butylcalix[4]arene and its derivatives, viz., *p-tert*-butylphenol and formaldehyde, were procured from a US commercial supplier, and the other chemicals, viz., NaOH, $LiAlH_4$, MnO_2, K_2CO_3, and the solvents, viz., acetone and diethyl ether, were purchased from a commercial supplier in India.

Solvents. All the solvents used were dried and distilled by usual procedures immediately before use. For the purification of methanol, 50−100 mL of analytical (AR)-grade methanol was first treated with 10 g of magnesium turnings and 1.0 g of iodine in a flask until the iodine disappeared and all of the magnesium was converted to the methoxide. An additional 2 L of methanol was added and the mixture refluxed for 2−3 h followed by distillation under nitrogen atmosphere immediately before use. Chloroform was also purified before use by treating AR-grade

chloroform with $CaCl_2$ followed by distillation under nitrogen atmosphere.

Details of Solution Studies. Bulk solutions of H_2L and the metal salts were made in $CHCl_3$ and MeOH, respectively, at 6×10^{-4} M. All the fluorescence titrations were carried out in 1 cm quartz cells by using 50 μL of H_2L, and the total volume in each measurement was made to 3 mL to give a final concentration of the ligand as 10 μM (i.e., the 3 mL solution contains 2.950 mL of CH_3OH and 0.050 mL of $CHCl_3$). During the titration, the concentration of metal perchlorate was varied accordingly to result in requisite mole ratios of metal ion to H_2L, and the total volume of the solution was maintained at 3 mL in each case by addition of CH_3OH. For absorption studies, the final concentration of [H_2L] was kept constant at 20 μM, and the procedure used for the titrations was the same as that used for fluorescence titrations. The bulk solution of anions, amino acids, and nucleotides were made by dissolving the corresponding compound initially in ~500 μL of deionized water and was diluted by using methanol to reach a final volume of 10 mL. During the titration, the in situ prepared H_2L (50 μL) and Zn^{2+} (100 μL) of 6×10^{-4} M were titrated against different mole ratios of anions, amino acids, and nucleotides in methanol by maintaining a total volume of 3 mL through out the experiment. A 100 μL portion of H_2L and Zn^{2+} of 6×10^{-3} M has been used for ESI MS titration studies after dilution by at least 1000-fold or higher. ^{1}H NMR titrations were carried out by dissolving 5 mg of H_2L in 400 μL of $CDCl_3$.

Synthesis and Characterization of 2[11]**.** To a solution of NaOH (5.0 g, 125 mmol) in H_2O (150 mL) was added 4-*tert*-butylphenol (19.0 g, 125 mmol), and a clear solution was obtained after heating. A 37% formaldehyde (19 mL, 250 mmol) solution was added dropwise under mechanical stirring after the reaction mixture was cooled to 0 °C. The mixture was stirred at room temperature for 7 days. The precipitate formed after the addition of NaCl (30 g) was filtered and suspended in 300 mL of water. The suspension was cooled, and 5% aqueous HCl was added. The resulting suspension was extracted with CH_2Cl_2 (150 mL × 3 times), and the combined organic phases were dried over anhydrous sodium sulfate. The product was purified by silica gel column chromatography using petroleum ether and ethyl acetate as eluent (6:4): yield (16.0 g, 60%); ^{1}H NMR ($CDCl_3$,δ ppm) 1.27 (s, 9H, C(CH_3)$_3$), 2.74 (s, 2H, CH_2OH), 4.76 (s, 4H, CH_2OH), 7.06 (s, 2H, Ar-*H*).

Synthesis and Characterization of 3[11]**.** A mixture of **2** (5.0 g, 25 mmol) and MnO_2 (22.0 g, 250 mmol) in $CHCl_3$ (150 mL) was stirred at room temperature for 8 h. After filtration, the product was purified by silica gel column chromatography using petroleum ether and ethyl acetate as eluent: yield (1.5 g, 30%); ^{1}H NMR ($CDCl_3$, δ ppm) 1.33 (s, 9H, C(CH_3)$_3$), 2.42 (t, 1H, CH_2OH, J = 6.5 Hz), 4.76 (d, 2H, CH_2OH, J = 6.3 Hz), 7.47 (d, 1H, Ar-*H*, J = 2.4 Hz), 7.62 (d, 1H, Ar-*H*, J = 2.4 Hz), 9.9 (s, 1H, Ar-O*H*), 11.22 (s, 1H, Ar-C*H*O).

Synthesis and Characterization of 5[10a]**.** A mixture of *p-tert*-butylcalix[4]arene, **4** (1.0 g, 1.55 mmol), K_2CO_3 (0.85 g, 6.20 mmol), NaI (0.92 g, 6.13 mmol), and chloroacetonitrile (0.4 mL, 5.33 mmol) in 50 mL of acetone was refluxed under nitrogen atmosphere for 7 h. The reaction mixture was allowed to cool down to room temperature and filtered through Celite and washed the Celite with dichloromethane to obtain light brown clear solution. This was concentrated to give a brown solid, which was recrystallized from chloroform/methanol to give a white crystalline solid: yield (900 mg) 80%; FTIR (KBr, cm^{-1}) 1482 (ν_{CN}), 3515 (ν_{OH}); ^{1}H NMR ($CDCl_3$, δ ppm) 0.88, (s, 18H, C(CH_3)$_3$), 1.32 (s, 18H, C(CH_3)$_3$), 3.45 (d, J = 13.55 Hz, 4H, Ar-CH_2-Ar), 4.22 (d, J = 13.55 Hz, 4H, Ar-CH_2-Ar), 4.81 (s, 4H, OCH_2), 6.73 (s, 4H, Ar-*H*), 7.12 (s, 4H, Ar-*H*). Anal. Calcd for $C_{48}H_{58}N_2O_4$: C, 79.30; H, 8.04; N, 3.85. Found: C, 79.49; H, 8.30; N, 3.92.

Synthesis and Characterization of 6. To a vigorously stirred solution of **5** (0.58 g, 0.81 mmol) in 32 mL of diethyl ether was added $LiAlH_4$ (0.25 g, 7.13 mmol) , and the reaction mixture was refluxed for 5 h. After that, the reaction flask was immersed into an ice−water bath, and excess $LiAlH_4$ was destroyed by the addition of wet benzene into the reaction mixture. The clear organic layer was decanted, and the inorganic salts were rinsed with benzene. The combined organic layers were evaporated to dryness to yield diamine as a light yellow solid: yield (470 mg) 85%; FTIR (KBr, cm^{-1}) 3362 ($\nu_{OH/NH}$); ^{1}H NMR ($CDCl_3$, δ ppm) 1.10 (s, 18H, C(CH_3)$_3$), 1.24 (s, 18H, C(CH_3)$_3$), 3.29 (t, J = 4.76 Hz, 4H, NCH_2), 3.37 (d, J = 12.82 Hz, 4H, Ar-CH_2-Ar), 4.07 (t, J = 4.76 Hz, 4H, OCH_2), 4.32 (d, J = 12.82 Hz, 4H, Ar-CH_2-Ar), 6.97 (s, 4H, Ar-*H*), 7.04 (s, 4H, Ar-*H*); ^{13}C NMR ($CDCl_3$, 100 MHz, δ ppm) 31.3, 37.8 (C(*C*H$_3$)$_3$), 34.0, 34.3 (*C*(CH$_3$)$_3$), 32.3 (Ar-*C*H$_2$-Ar), 42.7 (*C*H$_2$N), 78.7 (O*C*H$_2$), 125.6, 126.0, 127.8, 133.3, 142.2, 147.7, 149.3, 150.4 (Ar-*C*); ES MS m/z 735.26 (M$^+$, 100). Anal. Calcd for $C_{48}H_{66}N_2O_4$: C, 78.43; H, 9.05; N, 3.81. Found: C, 78.29; H, 8.87; N, 3.97.

Synthesis and Characterization of H_2L. A mixture of **6** (0.37 g, 0.53 mmol) and **3** (0.22 g, 1.06 mmol) was stirred in methanol (75 mL) at room temperature for 12 h followed by refluxing for 6 h. A yellow solution thus formed was concentrated, and the product was recrystallized in hexane: yield (49%, 0.29 g); FTIR (KBr, cm^{-1}) 1641 ($\nu_{C=N}$), 3394 (ν_{OH}); ^{1}H NMR:($CDCl_3$, δ ppm) 0.92 (s, 18H, C(CH_3)$_3$), 1.25 (s, 18H, C(CH_3)$_3$), 1.26 (s, 18H, C(CH_3)$_3$), 3.27 (d, 4H, Ar-CH_2-Ar, J = 13.44 Hz), 4.08 (t, 4H, OCH_2, J = 5.20 Hz), 4.20−4.26 (m, 8H, Ar-CH_2-Ar and NCH_2), 4.64 (s, 4H, CH_2OH), 6.76 (s, 4H, Ar-*H*), 7.00 (s, 4H, Ar-*H*), 7.12 (s, 2H, Ar-O*H*), 7.22 (d, 2H, Ar-*H*, J = 2.42 Hz), 7.29 (d, 2H, Ar-*H*, J = 2.35 Hz), 8.61 (s, 2H, C*H*=N), 13.64 (s, 2H, Ar-O*H*); ^{13}C NMR ($CDCl_3$, 100 MHz, δ ppm) 31.1, 31.5, 31.8 (C(*C*H$_3$)$_3$), 31.8 (Ar-*C*H$_2$-Ar), 33.9, 34.0, 34.1 (*C*(CH$_3$)$_3$), 58.5 (N*C*H$_2$), 62.4 (O*C*H$_2$), 75.3 (*C*H$_2$OH), 117.8, 125.2, 125.7, 127.5, 127.7, 128.2, 129.3, 132.5, 141.0, 141.6, 147.3, 149.6, 150.5, 157.7 (Ar-*C*), 168.18 (N*C*H); ES MS m/z 1115.77 (M$^+$, 70). Anal. Calcd for $C_{72}H_{94}N_2O_8.C_2H_5OH$: C, 76.51; H, 8.68; N, 2.41. Found: C, 76.98; H, 8.34; N, 2.34.

Acknowledgment. C.P.R. acknowledges financial support by DST, CSIR, and BRNS-DAE. R.J. thanks UGC and J.P. C. thanks CSIR for their research fellowships. We thank SAIF, IIT Bombay, for ESI MS measurements.

Supporting Information Available: Spectral data of L, fluorescence data, minimum detection limit, computational data, absorption data, and pie chart. This material is available free of charge via the Internet at http://pubs.acs.org.